# INFN - Laboratori Nazionali di Frascati

Servizio Documentazione

---

**LNF-87/24(P)**

12 Giugno 1987



S. Tazzari:


**ELECTRON STORAGE RINGS FOR THE PRODUCTION OF SYNCHROTRON RADIATION**


Lecture given at the
Joint U.S. - CERN Topical Course
"Frontiers of Particle Beams"
South Padre Island Texas, October 23-29, 1986



**Servizio Documentazione**
dei Laboratori Nazionali di Frascati
P.O. Box, 13 - 00044 Frascati (Italy)

INFN - Laboratori Nazionali di Frascati
Servizio Documentazione

LNF-87/24(P)
12 Giugno 1987

# ELECTRON STORAGE RINGS FOR THE PRODUCTION OF SYNCHROTRON RADIATION

S. Tazzari
INFN - Laboratori Nazionali di Frascati, P.O. Box 13, 00044 - Frascati (Italy)

## 1. INTRODUCTION

Intense, polarized photon beams, ranging in energy all the way from the infrared to the hard X-ray region are obtained from electron storage rings and are finding application in an ever increasing number of branches of science and technology.

The first synchrotron radiation (SR) users, back in the sixties, used (parasitically) the radiation from the bending magnets of HEP colliding beam facilities. However, with the development of the field, dedicated storage rings started to be built and novel radiation sources, such as wiggler magnets and undulators, were developed with dramatic improvements in beam quality and reliability.

A large number of SR sources are in operation, or under design, all over the world.

## 2. PHYSICS AND EXPERIMENTAL REQUIREMENTS

The distribution of interest in synchrotron radiation over the various scientific disciplines[1] is shown in Fig. 1. The frequency of utilization of different experimental techniques is also given on the same figure. Most SR users are found in the fields of: Basic condensed matter physics, Materials science and technology, Biology, Biophysics and Medicine.

The most exciting developments are connected with obtaining extremely high spatial and time resolutions. Very small samples containing few atoms, and the evolution of chemical reactions and biological phenomena, can thus be studied and followed in real time.

Synchrotron radiation users are concerned with a wide range of phenomena, and a large number of experiments many of which need very fast data acquisition rates (i.e. for kinetic studies), high time resolution and possibly the use very small samples, are carried out n parallel at any given facility.

The general specifications for the source are therefore that it should be:

- Flexible (providing for variable wavelength , adjustable source size, etc.)
- Reliable
- Highly intense
- Highly (spectrally ) bright and brilliant.

Concerning brightness and brilliance, note that the great majority of experiments requires that:

a) the largest possible number of photons in the desired energy bin reach the sample in any given time interval, so that samples containing fewer and fewer atoms (dilute solutions, very small biological samples/crystals, monoatomic surface layers, dynamic behaviours,...) can be studied.

b) the photons reaching the sample have the smallest possible angular divergence (diffraction is often involved).

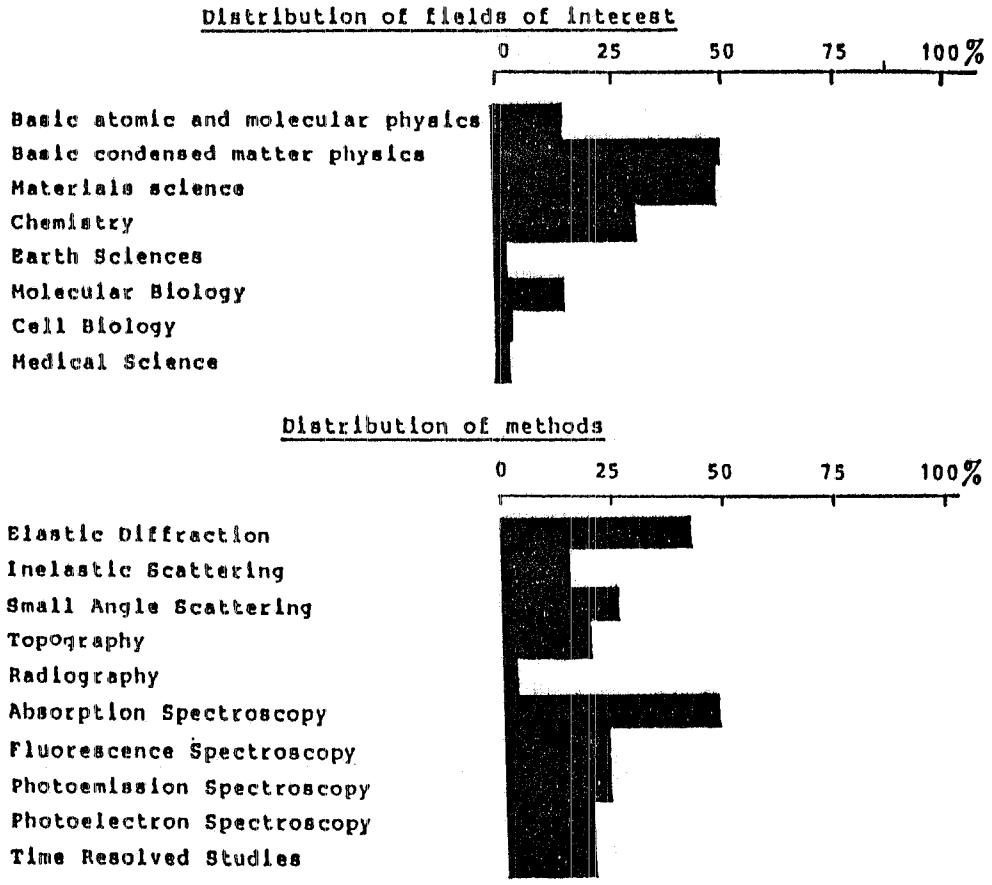


**FIG. 1** Science with Synchrotron Radiation

For an unfocused beam this translates into the requirement of high spectral brightness, $B_\Omega$

$$B_\Omega = d^3n /[dt\, d\Omega\, (\Delta\lambda/\lambda)] \qquad (1)$$

where n is the number of photons, $\Omega$ the solid angle and $(\Delta\lambda/\lambda)$ the wavelenght relative bandwidth.

For a focused beam it translates into the requirement of high spectral brilliance, $B_r$

$$B_r = d^4n /[dt\, d\Omega\, ds\, (\Delta\lambda/\lambda)] \qquad (2)$$

where s is the source size.

## 2.1. Evolution of Source Performances

An increasing emphasis is being put by the users on obtaining very brilliant sources through the use of very low emittance, high current storage rings and the implementation of a variety of insertion devices to generate the desired radiation. The time evolution of the brilliance of X-ray sources[2] is shown in Fig. 2. In Fig. 3 the wavelength range and the brilliance and flux of some of the existing or presently being designed sources is shown as an example, to gain a feeling for the orders of magnitude.

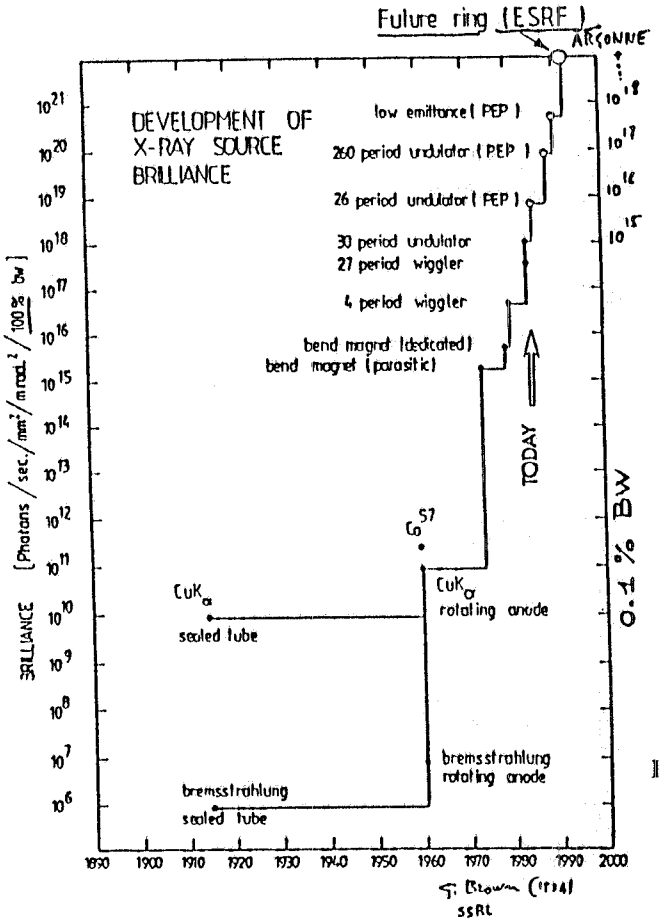


FIG. 2 Development of X-ray source brillance

## 3. THE PRODUCTION OF SYNCHROTRON RADIATION

### 3.1. Bending Magnet Sources

The basic geometrical characteristics of a bending magnet source are illustrated in Fig. 4. Since the vertical angular aperture of the emerging radiation fan ($\theta_v \approx 1/\gamma$) is much smaller than the radial one the number of photons, per unit time and per unit solid angle, is often integrated over the vertical distribution giving the total flux, $\Phi_T$:

$$\Phi_T = d^2n / d\theta_r\, dt \tag{3}$$

or the spectral flux

$$\Phi = d^2n / [d\theta_r\, dt\, (\Delta\lambda/\lambda)\,] \tag{4}$$

where $\theta_r$ is the horizontal aperture angle of the radiation. The spectral flux is usually called flux for short; in the following the 'spectral' will be dropped from all definitions. Because of the vertical collimation and the small effective source size a bending magnet source is intrinsically much more brilliant than an X-ray tube. An example of the phase space distribution of a bending magnet source[3], showing the equal intensity contours is given in Fig. 5. while the spectrum of the radiation is shown in Fig. 6. A critical energy $\varepsilon_c$ is defined that divides the power spectrum into two equal halves:

$$\varepsilon_c = h\,\nu_c = (3/8\pi^2) h\,c(\gamma^3/\rho_o) = (3/8\pi^2)(h\,e/m_o)\,\gamma^2\,B_o \qquad (5)$$

where h is the Planck constant, $\gamma$ the usual relativistic normalized energy of the electron beam and $\rho_o$ the bendig radius in the magnet , $B_o$ the bending field and $m_o$ the electron rest mass.

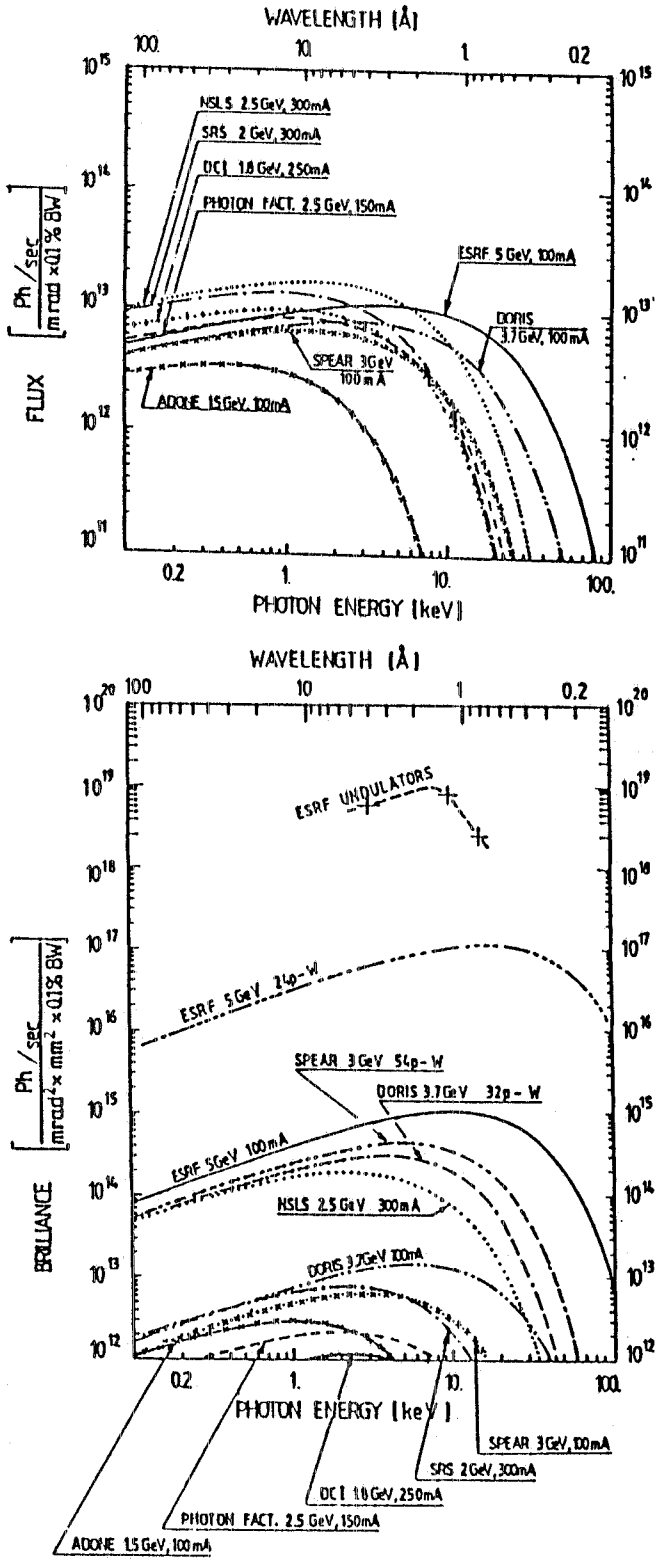


FIG. 3 FLUX brillance for some of the existing sources compared to the design values for the ESRF

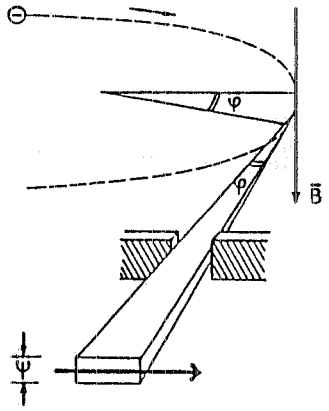


FIG. 4 Geometrical characteristics of a bending magnet source

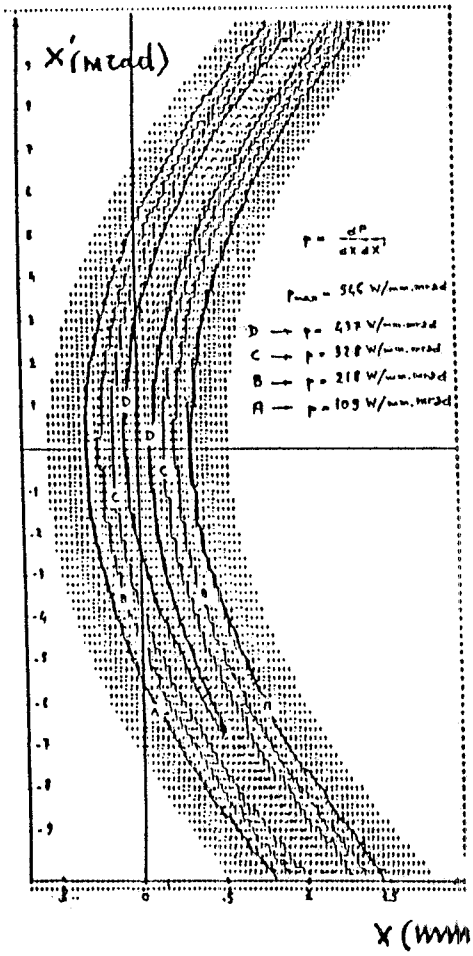


FIG. 5 Phase space distribution of the ESRF bending magnet source

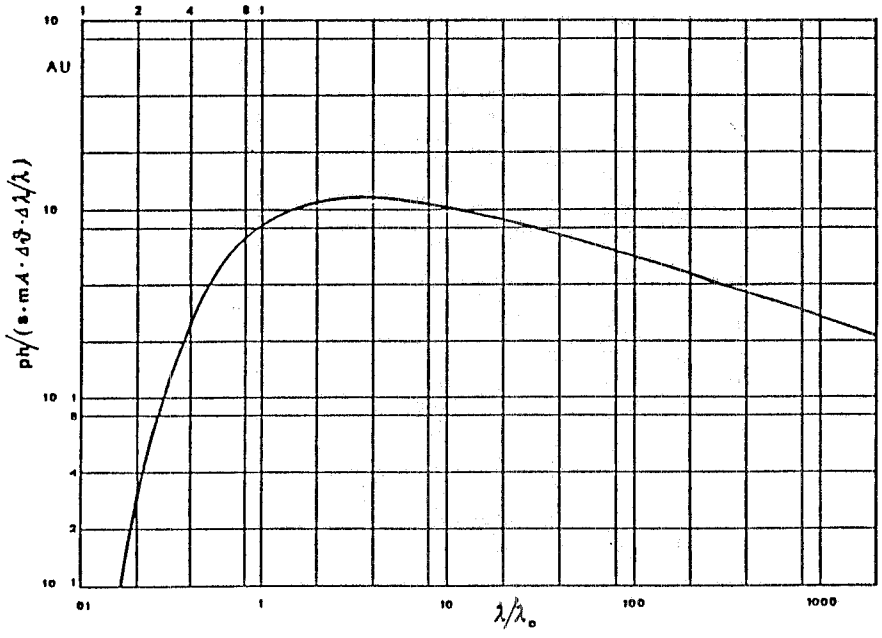


FIG. 6 Spectrum of the radiation from a bending magnet

A simple explanation[4] for the parameter dependence of the critical energy can be worked out by looking at Fig. 7. The observer sees a light pulse that is $\Delta t$ long in time, where $\Delta t$ is the difference between the time taken by the electron to travel along the curved trajectory and that along the chord corresponding to an arc subtending an angle of about $1/\gamma$. One has:

$$\Delta t \approx 4\,\rho_o /(3\,c\,\gamma^3)$$

so that

$$\varepsilon_{typ} = h/\Delta t \approx (3/4)\; h\,c\,(\gamma^3/\rho_o).$$

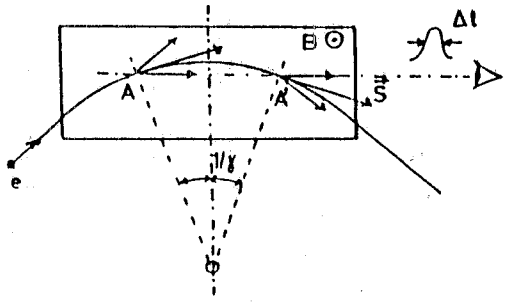


FIG. 7 Light pulse seen by observer

For any given machine the radius of curvature of the bending magnet is a fixed quantity. The critical energy of the radiation can therefore only be changed, for all users, by changing the operation energy (generally an unpopular operation !). The brilliance is also fixed so that increasing the acceptance angle of the experiment will only increase the flux. This situation can be improved upon by inserting "Wiggler" magnets in the storage ring straight sections.

### 3.2. Wiggler Sources

A wiggler is an alternating field magnet. An example of the field[5] in an actual many-pole wiggler is shown in Fig. 8a. In order for the storage ring to remain (to first order) unperturbed, the field integral over the wiggler length must vanish. However the field in the device can now be controlled, and so can the value of $\varepsilon_c$, independent (at least to some extent) on the storage ring energy. If the main purpose of the insertion device is that of shifting $\varepsilon_c$, it is called a "wavelength shifter" (WLS). It will usually have a single period and a single high field pole. An example, a design for a superconducting wavelength shifter, is shown in Fig. 9. The additional reverse field poles are only used to make the field integral zero and are generally, although not always, designed to have a lower field. If flux and brilliance are also to be increased a many-pole wiggler is the preferred solution. When it has N periods, flux and brilliance are approximately proportional to N. It should be added that, as a further approximation , other considerations and parameters such as the ring energy, the source size and shape,etc will often influence the choice (see below).

For a sinusoidal magnetic field the trajectory is approximately sinusoidal (Fig. 8b ).

Let

$$B = B_o \sin(2\pi s/\lambda_o) \qquad (6)$$

and define:

$$K = (e\, B_o \lambda_o)/(2\,\pi\, m_o\, c), \tag{7}$$

the full angular aperture of the radiation beam is then:

$$\theta_M \approx 2\,K/\gamma \tag{8}$$

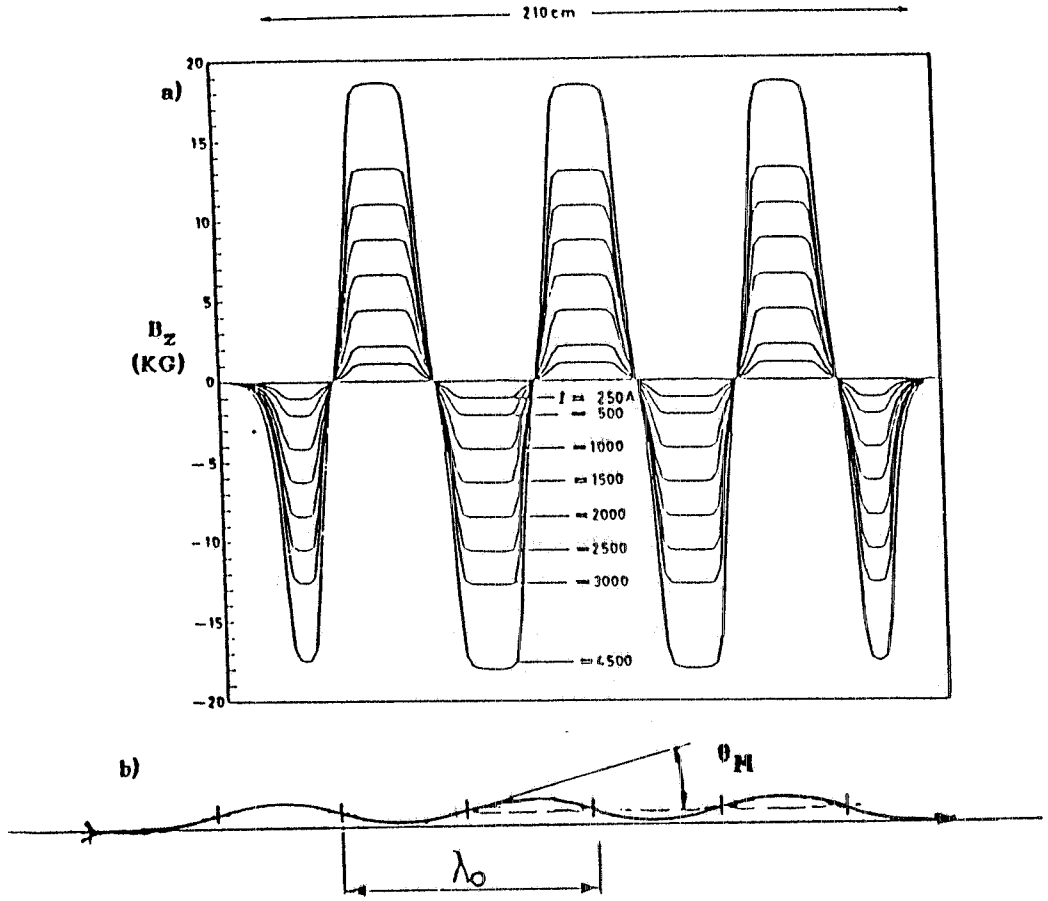


**FIG. 8** a) Many-pole wiggler. Maps of B along the longitudinal axis at magnet midplane, for various supply currents. b) Schematic trajectory in a many-pole wiggler. $\theta_M$ is the maximum emission angle.

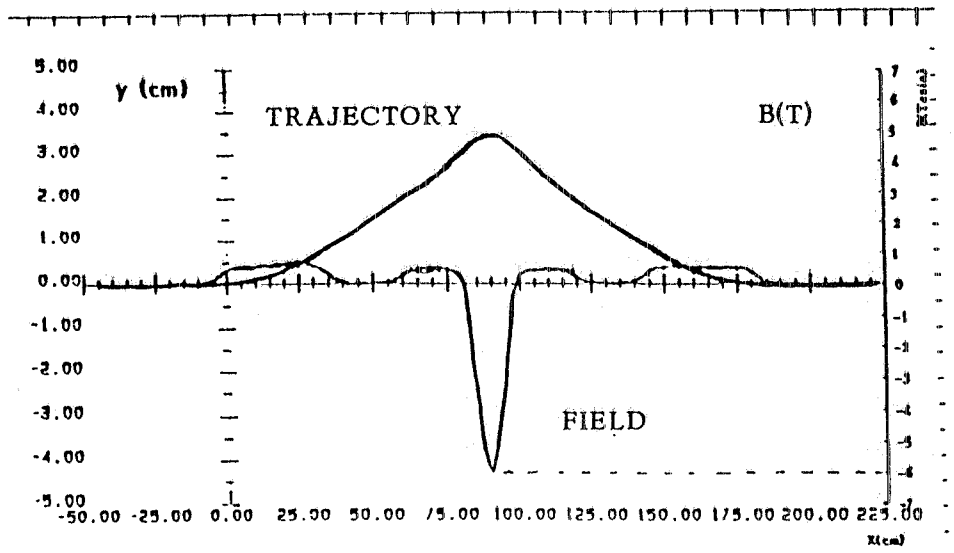


**FIG. 9** A superconducting wavelength shifter with low field compensating poles

For a typical wiggler magnet, by definition: $K \gg 1$. The radiation cone is, therefore, still much wider than the natural emission angle ($1/\gamma$) but can now be controlled through $B_o$ and $\lambda_o$.

The overall power radiated by a current I in a wiggler with N periods is given by:

$$P_W = (\pi e / 3 \varepsilon_o)\,(K^2 N / \lambda_o)\, I\, \gamma^2 \qquad (9)$$

where $\varepsilon_o$ is the dielectric constant of vacuum. In practical units:

$$P_{W\,(Kw)} = .634\, E^2_{(GeV)}\, B_o^2{}_{(T)}\, N\, l_{o\,(m)}\, I_{(A)}. \qquad (9')$$

The number of photons per unit relative energy bin can be roughly estimated by dividing $P_W$ through $e_c$. In fact the exact formula is[4]:

$$dn/(dt\, d\varepsilon/\varepsilon) = (P_W/\varepsilon_c)\, S(\varepsilon/\varepsilon_c) = A_n K N I \qquad (10)$$
$$A_n = (4\pi^2 e / 9 \varepsilon_o hc)\, S(\varepsilon/\varepsilon_c)$$

where $S(\varepsilon/\varepsilon_c)$ is the well known SR energy distribution function ( see Fig. 6).

In order to again roughly estimate flux we divide (10) by $\theta_M$, the horizontal aperture, and to estimate brightness by $1/\gamma$, the vertical aperture. We obtain:

$$\Phi \approx N I \gamma \quad ; \quad B_\Omega \approx N I \gamma^2 \qquad (11)$$

Note that K has dropped out of the expressions. Exact expressions can be found in Ref. [4].

### 3.3. **Plane Undulators**

When K is made $\leq\approx 1$ the aperture of the radiation fan due to the 'wiggles' in the trajectory becomes comparable to the natural radiation aperture and interference effects start to appear. The continuous radiation spectrum evolves towards a line spectrum containing a series of harmonics at wavelengths given (for a sinusoidal field) by :

$$\lambda_i = \lambda_o (1 + K^2/2 + \gamma^2\theta^2) / (2i\gamma^2) \quad i=1,2,3,..... \qquad (12)$$

where $\lambda_o$ is the magnetic field spatial wavelength, i the harmonic number and $\theta$ the observation angle. The intensity pattern is such that at exactly $\theta = 0$ only the odd harmonics are present.

The total emitted power is given by

$$P_t = h_t I_b \gamma^2 N \lambda_o K^2 = h_t I_b \gamma^2 L_u K^2 \qquad (13)$$

with: $h_t = 1.9\ 10^{-6}$ w/A/m , and $I_b$ the beam current. Since $K \approx 1$, $P_t$ is always lower than the power radiated by a wiggler of the same length. The spectral flux at the peak of the $i^{th}$ harmonic - i.e. at

$\lambda_p = \lambda_i(1+1/iN)$ - is given in Ref. [6,7]:

$$\Phi_i = h_\Phi \, I \, N \, U_i \qquad (14)$$

with $h_\Phi = 1.43\ 10^{14}$ photons/s/.1%/A and $U_i$ a universal function of K. $\Phi_i$ can be higher than that for a wiggler of the same length. $U_i$ can be expressed as a function of $(\lambda / \lambda_f)$ with $\lambda_f = \lambda_o/(2\gamma^2)$.

For a pointlike electron beam the spectral brightness is

$$B_\Omega = h_b \, N^2 \, \gamma^2 \, I_b \, F_i(K,\theta,\varphi) \qquad (15)$$

where $F_i(K)$ is a function containing a line shape function ($sinc^2$) and an angular distribution function[6].

For a real electron beam the situation is more complicated. As N increases the radiation beam angular divergence starts to be dominated by the electron beam one and the $N^2$ dependence tends to become a simple N dependence. Similar formulae can be derived for helical undulators[7].

### 3.3.1. Polarisation

In a plane undulator the polarisation of the radiation is linear, in the plane perpendicular to the magnetic field. In a helical one it is circular. Circular polarization can also be obtained, at least in a certain range of beam energies, by a sequence of crossed, properly spaced plane undulators [8,9] or 'asymmetric' wigglers [10].

## 3.4. Undulator Design Constraints

The values of $B_o$ and $\lambda_o$ (and therefore of $\lambda$ and K) that can in practice be obtained depend on the permanent magnet material and on the gap. They can be computed from a semi empirical formula derived by K.Halbach[11,12]:

$$B_o = B_M \exp\left( -\xi \, [b - c\,\xi] \right) \quad ; \quad \xi = g/\lambda_o \qquad (16)$$

where g is the allowed gap (the formula is valid for $\approx .7 > \xi > \approx .07$ ). For "hybrid" undulators built of SmCo permanent magnet blocks (the equivalent of coils) together with high permeability steel poles (e.g. Vanadium Permendur), one has:

$$B_M = 3.33\ T \quad ; b=5.47 \; ; \quad c = 1.8$$

while for pure SmCo magnets

$$B_M = 1.1\ T \quad ; b=3.14 \; ; \quad c = 0$$

### 3.5. Effective Source Size

The radiation is produced by an electron beam that has a finite size in the four dimensional transverse phase space (x,x', z,z'). The electron beam is gaussian and its envelope is an ellipsoid with standard deviations $\sigma_x$ , $\sigma_{x'}$ , $\sigma_z$ , $\sigma_{z'}$. On the other hand, even for an electron beam that is pointlike in phase space, because of the limited angular aperture of the emitted waves, the minimum radiation source size that can be reconstructed is diffraction limited.

From the uncertainty principle it is easy to deduce that the minimum resolvable phase space area for a radiation beam with wavelength $\lambda$ is:

$$\Delta x \, \Delta x' = \Delta z \Delta z' = \sigma_R \, \sigma_{R'} \approx \lambda/2\pi \tag{17}$$

having defined (for the sole purpose of estimating widths) standard deviations ($\sigma_R$ $\sigma_{R'}$) also for the radiation beam. In reality photon distributions are generally not gaussian: for other than heuristic purposes this should be properly taken into account [13].

Coming back to the electron beam, in a storage ring the product

$$\varepsilon_x = \sigma_x \sigma_{x'} \tag{18}$$

is the betatron radial emittance and is a constant of motion determined by the lattice. The vertical emittance, $\varepsilon_z = \sigma_z \sigma_{z'}$ , is proportional to $\varepsilon_x$ through a coupling constant $0 \le k \le 1$ describing the coupling between horizontal and vertical oscillations. The value of $k$ can be controlled by the lattice tunes or by coupling elements such as tilted quadrupoles. It is zero for an ideal machine: its ultimate value in a real machine depends on machine errors and imperfections. It can be made much less than 1 (.1 to .001 ). The values of $\sigma_x$ and $\sigma_z$ are of course functions of the position along the machine. At places such as the long straight sections where the Twiss functions $\alpha_x$, $\alpha_z$, are zero one has:

$$\begin{aligned} \varepsilon_x &= \sigma_x(\sigma_x/\beta_x) = \sigma_x^2/\beta_x \\ \varepsilon_z &= k\,\varepsilon_x = \sigma_z \sigma_{z'} = \sigma_z^2/\beta_z. \end{aligned} \tag{19}$$

By properly choosing the $\beta$ functions at the radiation source points one can therefore change the shape of the phase space ellipse, in particular trade beam dimensions for divergence and vice versa. By keeping $k$ small, a much smaller emittance can be achieved in the vertical than in the horizontal plane.

In analogy to the electron beam, the radiation beam can be described by an emittance

$$\varepsilon_R = \sigma_R \, \sigma_{R'} \tag{20}$$

the same for both planes and also a constant. In particular, for an undulator of length L, at the harmonic central wavelength $\lambda_i = (1+K^2/2)\,\lambda_o/2\gamma^2$, one has:

$$\sigma_R' \approx (\lambda/L)^{1/2} \quad (21)$$

so that

$$\sigma_R \approx (1/2\pi)(\lambda L)^{1/2}. \quad (22)$$

The angular distributions being different for different $\lambda$ and in general not gaussian, the above definitions are only approximate. Definitions differing by factors of two and applying to slightly different cases are often found in the literature.

The effective source size in phase space $(\Sigma_x, \Sigma'_x, \Sigma_z, \Sigma'_z)$ is determined by the convolution of the two distributions:

$$\Sigma = (\sigma^2 + \sigma_R^2)^{1/2} \quad ; \quad \Sigma' = (\sigma'^2 + \sigma_R'^2)^{1/2} \quad (23)$$

and since

$$\sigma^2 = \varepsilon \beta \quad ; \quad \sigma'^2 = \varepsilon/\beta \quad (24)$$

there is a (very broad) optimum for $\beta$, the same in both planes:

$$\beta_{opt} = \sigma_R/\sigma_R'.$$

It is often useful to have a beam with the smallest possible angular divergence: $\sigma'$should then be much smaller than $\sigma_R'$. Undulators are therefore often placed in "high $\beta$" straight sections.

For wigglers, wavelength shifters and bending magnet sources the beam angular spread plays hardly any role because it is usually much smaller (at least in one plane) than the aperture of the radiation fan produced by the curvature in the trajectory. The main objective is then to achieve a small source size, i.e. to have $\sigma \ll \sigma_R$. This calls for a low $\beta$ at the wiggler location. A low $\beta$ also helps in reducing the effects of these strong field magnets on the machine optics. The shape of the source in phase space has however to be watched. A strong wiggler may produce a large amplitude wiggler in the trajectory and the source intensity distribution in phase space may consequently become very complicated. An example[14] is shown in Fig. 10.

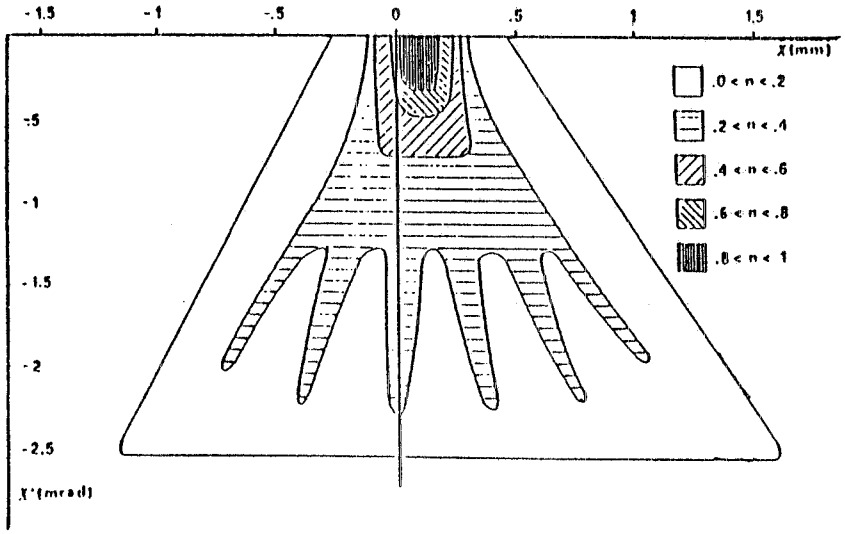


**FIG. 10** - Intensity distribution in phase space for a high K wiggler.

### 3.6. Undulator Tunability

The undulator spectrum can be shifted by changing the magnetic field: i.e. for a permanent magnet device by changing the gap. For a fixed minimum gap, the range over which the central wavelength can be varied while maintaining an acceptable flux increases with energy. However K varies with wavelength and the surface power density in an undulator beam line increases approximatively in proportion to $E^4$.

## 4. LOW EMITTANCE LATTICES

### 4.1. The Electron Beam Emittance

The primary requirement for high brilliance is to have a low emittance electron beam. This is of course useful only as long as

$$\varepsilon >\approx \varepsilon_R .$$

In practice, however, this condition is always met by hard X-ray machines for which the required wavelengths are in the order of 1 Å or less , so that $\varepsilon_R = \lambda/(2\pi) \leq \approx 2\ 10^{-11}$ m·rad, a value much smaller than electron emittances achievable in today's state of the art SR machines.

The horizontal betatron emittance, $\varepsilon_o$, usually called emittance for short, is given by:

$$\varepsilon_o = (C_q \gamma^2/J_x)\cdot(\int |G^3| H\ ds)/(\int G^2 ds) \qquad (25)$$

with $G = 1/\rho = ecB/E = e\cdot B/(mc\cdot\gamma)$ and
$C_q = 3.832\ 10^{-13}$ m

where $\rho$ is the bending radius produced by the magnetic field B on an electron of energy E, m is the electron rest mass, and

$$H = (1+\alpha^2]\ D_x^2/\beta_x + 2\ \alpha\ D_x D'_x + \beta_x D'^2_x \qquad (26)$$

is the lattice 'invariant', with $D_x$ the dispersion function and $\alpha$, $\beta$ the Twiss functions. By defining:

$$I_5 = \int |G^3| H\ ds = \int [e/(mc\gamma)]^3 \cdot |B|^3 H\ ds\ , \qquad (27)$$
$$I_2 = \int G^2\ ds = \int [eB/(mc\gamma)]^2\ ds.$$

the emittance becomes

$$\varepsilon_o = (C_q\ \gamma^2/\ J_x)(I_5/I_2). \qquad (28)$$

For an isomagnetic lattice , for which $B=B_o$ and $\rho = \rho_o$ in the bending magnets are positive

constants, $I_5$ and $I_2$ are given by:

$$I_5 = 2\pi \langle H \rangle / \rho_0^{\,2} \quad , \quad I_2 = 2\pi / \rho_0 \tag{29}$$

where the < > indicates the average over the bending magnets. The emittance then becomes:

$$\varepsilon_0 = ( C_q \gamma^2 / J_x)( \langle H \rangle / \rho ) \tag{30}$$

Since, furthermore , $\langle H \rangle$ is proportional to $\rho_0$ it is found that $\varepsilon_0$ does not depend on the value of $\rho_0$. Note that:

$$\varepsilon_0 = \sigma_E^{\,2} \langle H \rangle (J_E/J_x) \tag{31}$$

In fact, for all lattices, the emittance can be expressed in the form:

$$\varepsilon_0 = (k_\varepsilon/J_x)\ \theta_B^{\,3}\ \gamma^2 \tag{32}$$
$$\theta_B = 2\pi/N_B$$

where $\theta_B$ is the magnet bending angle and $k_\varepsilon$ is a function of lattice parameters only, depending on the particular type of lattice. For the most commonly used lattices it is a constant. $N_B$ is the number of (identical) bending magnets in the ring.

### 4.1.1. Values of $k_\varepsilon$ for the Most Common Low Emittance Lattices with Uniform Field Bending Magnets

For most lattices the minimum achievable emittance can be computed analytically. For instance for a Chasman-Green type of lattice with Dx=D'x= 0 at the bending magnet entrance point (Double Bend Achromat, DBA)[15] one obtains:

$$K_\varepsilon = C_q/(4\sqrt{15}) = 2.48\ 10^{-14}\ \pi\text{m}.$$

If $D_x$ and $D'_x$ at the magnet entrance are adjusted to further minimize the emittance [16] one obtains:

$$K_\varepsilon = C_q/(12\sqrt{15}) = 8.24\ 10^{-15}\ \pi\text{m}.$$

Detailed studies of FODO lattices have also been carried out , leading to [17]:

$$K_\varepsilon = 1.55\ 10^{-13}\ \pi\text{m}$$

Other types of lattices , with uniform field or gradient magnets, have also been proposed, see for instance References [18,19,20].

In practice the theoretical absolute minima for the radial emittance of the various lattices are

rather difficult to achieve because of problems arising from the very strong focusing they require. It should be kept in mind that the lower the lattice emittance, the stronger are the sextupoles required to correct the lattice chromaticity (see Section 4.2.2). As a consequence the particle dynamics becomes highly nonlinear and the acceptance of the storage ring can be severely limited. A realistic lattice design therefore requires a considerable amount of work (tracking, etc.) before its acceptance, current, lifetime, and performance in general can be established.

In the range from 1 to 6 GeV , $\varepsilon_x / \gamma^2 \approx 10^{-17}$ m is close to the lower limit of existing designs for long lifetime, high current synchrotron radiation sources.

## 4.2. Problems Inherent to Low Emittance (l.e.) Lattices for SR Sources

### 4.2.1. General Remarks

To obtain very low emittances very strong focusing lattices have to be used. The strength of the aberrations - 'chromatic' or amplitude dependent - of a lens system increases, for a given aperture, with the strength of the individual lenses, requiring strong corrections and leading to a very nonlinear system of forces acting on the individual particle. Resonances of up to high order can be excited and eventually highly nonlinear motions, simulating a chaotic behaviour can result. In practice the effective acceptance of the machine will be reduced. The maximum aperture within which particles execute stable oscillations is, somewhat improperly, called 'dynamic aperture'. It can not usually be defined analytically but has to be found by time consuming simulations[21].

### 4.2.2. Chromaticity Correction

The natural linear chromaticity of a lattice, $\xi_T$ , defines the changes in the tune seen by an off momentum particle:

$$\xi_{Ti} = \Delta Q_i/(\Delta p/p) = \int \beta_i(s)\, K_i(s)\, ds \qquad (33)$$

where i =x,z and $K_i(s) = G_i(s)/(B\rho)$ is the strength of the quadrupole field along the particle trajectory. From Eq. (33) one sees that the largest contributions to $\xi_T$ come from quadrupoles located where $\beta$ is high. It is not unusual for l.e. lattices to have uncorrected values of $\xi_T \approx 100$, leading to an insufficient momentum acceptance.

In any one plane the chromaticity can be corrected by adding sextupolar fields that produce a tune shift with momentum given by:

$$[\Delta Q_i/(\Delta p/p)]_S = \xi_{Si} = -(1/4\pi) \int \beta_i(s)\, D_x(s)\, h_i(s)\, ds \qquad (34)$$

where $h_i(s) = G_{Si}(s)/(B\rho)$

$G_{Si}(s) = B_i''/(2a^2)$

and 'a' is the sextupole bore radius.

Note that for a sextupole the sign of h(s) is opposite in the two planes (x and z). Therefore, to correct both chromaticities at least two families of sextupoles are needed, one located where $\beta_x$ is higher than $\beta_z$ and one at places where the opposite is true.

Also note that since in l.e. lattices $D_x$ tends to be low, the sextupole strength h(s) needed to correct the chromaticity tends to be higher than for more usual lattices.

The strong sextupoles one has to introduce to correct the linear chromaticity produce nonlinear terms of their own in the particle trajectory. If following Ref. [22] one writes out the coordinates of a particle traversing one lattice superperiod to second order in x, z, $\Delta p/p$, one obtains:

$$\underline{X}_L = M_x \underline{X}_o + 2^{nd}\text{order terms } ( p^2; px_o;\ px'_o; x^2_o; x_o x'_o; x'^2_o; z_o^2;\ z_o z'_o; z'^2_o)$$
$$\underline{Z}_L = M_z \underline{Z}_o + 2^{nd}\text{order terms } ( pz_o;\ pz'_o; x^2_o; x_o z_o; x'_o z_o; x_o z'_o;\ x'_o z'_o) \qquad (35)$$

where $\underline{Y}$ is the vector $| y, y', \Delta p/p |$ ; $y = x,z$, and $M_y$ is the superperiod linear transfer matrix.

In order for the lattice to be perfectly corrected all (30) second order terms should be made to vanish and this in turn requires that the 18 integrals listed in Table I vanish. The 18 integrals are divided into groups according to their effect on the behaviour of the lattice parameters and functions, and to the resonances they excite. It is in practice impossible to exactly cancel all 18 of them.

**TABLE I** - Integrals relevants to the lattice behaviour with sextupoles (to $2^{nd}$ order in x, z, $\Delta p/p$).

| | |
|---|---|
| $I_1 = \int_o^L (2h\,D - K)\,\beta_x\,ds$<br>$I_4 = \int_o^L (2h\,D - K)\,\beta_z\,ds$<br>Ordinary chromaticity integrals<br>h: sextupole coefficient | $I_9 = \int_o^L h\,\beta_x^{1/2} \cos\mu_x\,ds$<br>$I_{10} = \int_o^L h\,\beta_x^{1/2} \sin\mu_x\,ds$<br>$I_{13} = \int_o^L h\,\beta_x^{1/2} \cos\mu_x\,ds$<br>$I_{16} = \int_o^L h\,\beta_x^{1/2} \sin\mu_x\,ds$<br>$I_{9,10,13,16}$ excite integer resonances |
| $I_7 = \int_o^L (h\,D - K)\,\beta_x^{1/2} \cos\mu_x\,ds$<br>$I_8 = \int_o^L (h\,D - K)\,\beta_x^{1/2} \sin\mu_x\,ds$<br>$I_{7,8}$ influence the off-momentum orbits | $I_{11} = \int_o^L h\,\beta_x^{1/2} \cos\mu_x\,ds$<br>$I_{12} = \int_o^L h\,\beta_x^{1/2} \sin\mu_x\,ds$<br>$I_{14} = \int_o^L h\,\beta_x^{1/2} \sin(\mu_x + 2\mu_z)\,ds$<br>$I_{15} = \int_o^L h\,\beta_x^{1/2} \sin(\mu_x + 2\mu_z)\,ds$<br>$I_{11,12,14,15}$ excite 3rd order resonances<br>$3Q_x = n$; $Q_x \pm 2Q_z = n$ |
| $I_2 = \int_o^L (2h\,D - K)\,\beta_x \cos 2\,\mu_x\,ds$<br>$I_3 = \int_o^L (2h\,D - K)\,\beta_x \sin 3\,\mu_x\,ds$<br>$I_{2,3}$ influence $(\partial/Q)/(\partial/p)$, $(\partial/\beta)/(\partial/p)$<br>$I_5 = \int_o^L (2h\,D - K)\,\beta_z \cos 2\,\mu_z\,ds$<br>$I_6 = \int_o^L (2h\,D - K)\,\beta_z \sin 2\,\mu_z\,ds$<br>$I_{5,6}$ excite 1/2 integer resonance $2Q_{x,z} = n$ | |

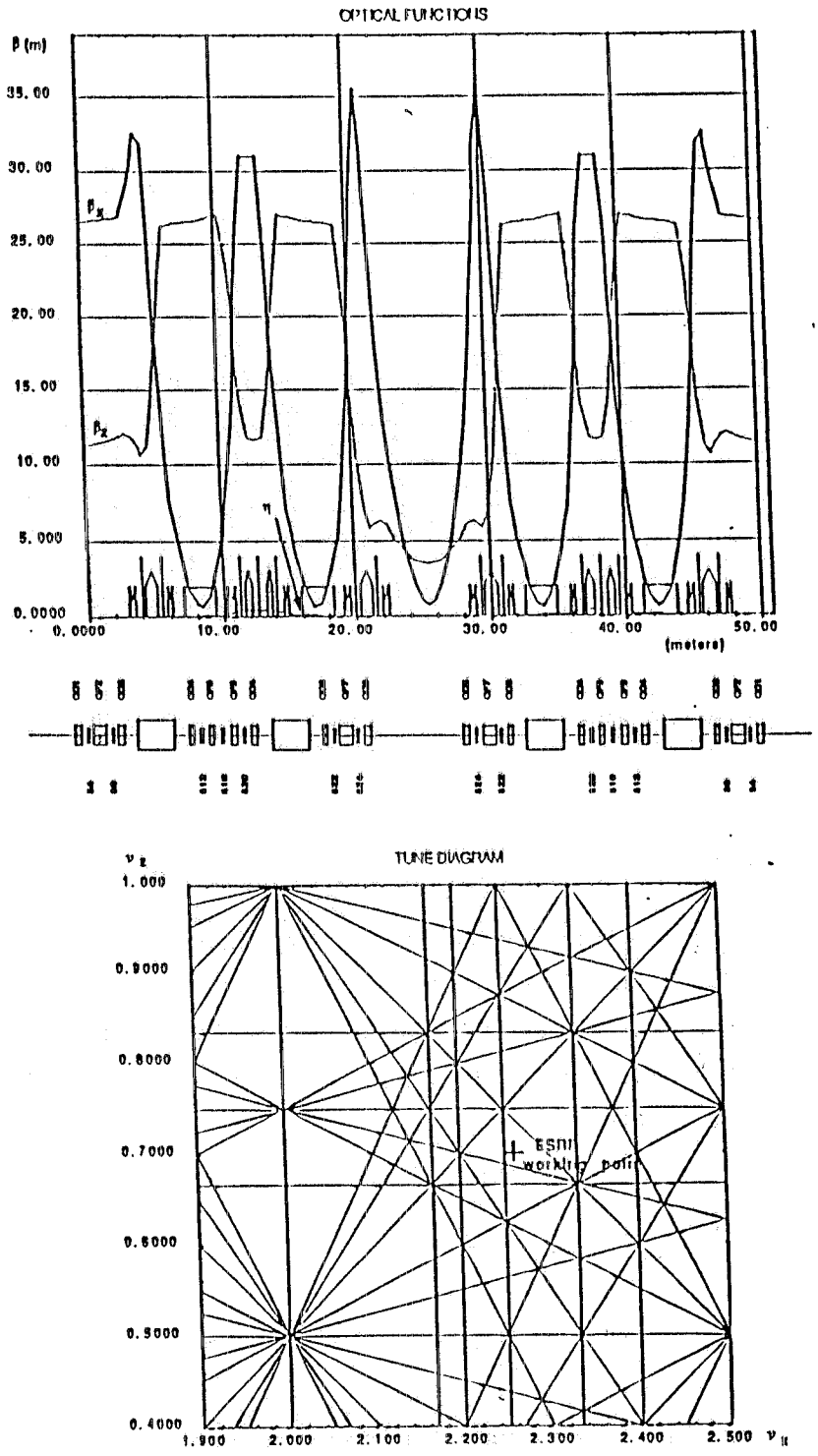


**FIG. 11** The ESFR lattice and tune diagram. The schematic layout of the lattice elements and the tune diagram are also shown

However the resonance driving integrals can be minimized by proper arrangements of sextupole families and by choosing a tune that is as far as possible from the resonance lines[23,24].

For the most extreme performance requirements higher order terms have also to be taken into account. In the design of the ESRF lattice[23] (see Fig. 12) resonances of up to sixth order had to be avoided.

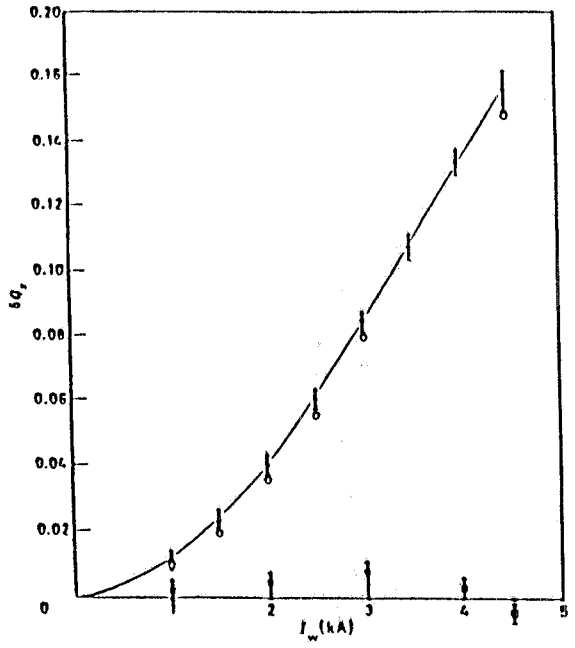


FIG. 12 Experimental betatron tune shift vs. wiggler current: * $\delta Q_z$, o $\delta Q_z^M$ rectangular model, ■ $\delta Q_x$.

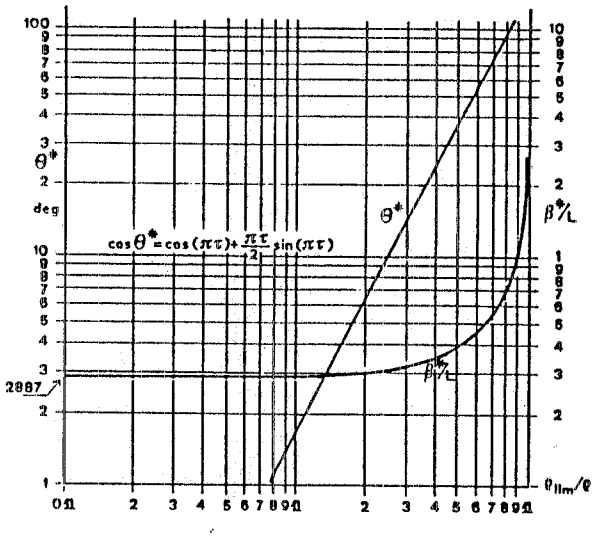


FIG. 13 $\vartheta^*$ and $\beta^*/L$ in the wiggler as functions of $\rho_{lim}/\rho$

### 4.2.3. Position and Field Errors

The lattice functions and parameters of a real machine are influenced by the inevitable position and field errors affecting the lattice elements. This is particularly important for low emittance lattices, since the lowest possible emittance is only obtained if the lattice functions in the bending fields are precisely tailored. Strong focusing and strong chromaticities also produce an extreme sensitivity to magnet positioning errors.

Typical state-of-the-art values for the magnet alignment errors $\Delta x$, $\Delta z$ and tilt $\Delta\alpha$ are:

$$\Delta x, \Delta z \approx 0.1 \text{ mm} \ , \ \Delta\alpha \approx 10^{-4} \text{ rad.}$$

With this kind of accuracy it is very likely that the closed orbit has to be corrected before a stable trajectory can be found.

Field errors can be systematic , such as differences between the ideal field shape and the actual shape obtained with a given pole profile, or random, such as field errors deriving from magnet assembly tolerances. Systematic errors are of course the same for all magnets of a type. Even relatively small errors can have a significant effect on the machine acceptance[25] ('dynamic aperture'). Random errors are usually more troublesome than systematic ones.

When designing a storage ring, the effect of errors and tolerances on the aperture has to be simulated by tracking.

The closed orbit is obtained ( provided the machine is stable ) by iteration:

$$\Delta \underline{Y}_o = A^{-1}( \underline{Y} - \underline{Y}_o) \qquad (36)$$

where $\underline{Y} = (x,x',z,z',\Delta p/p)$ , $\underline{Y}_o$ is the starting vector and A is the transfer matrix through one turn.

Special programs exist, such as PETROC [2] that allow one to simulate the correction of the closed orbit by means of beam position monitors and corrector dipoles.

## 4.3. Lifetime

### 4.3.1. Gas Scattering Lifetime

The scattering on the residual gas is important for low emittance machines even at relatively high energies when the physical or the 'dynamic' apertures are small. It is given by:

$$1/\tau_{sc} = c \sum_i N_i S_i \qquad (37)$$

with: $N_i = K n_i p_i$ ,
$K_n = 3.53\ 10^{16}$ molecules/cm$^3$/torr
$S_i = \int_\Omega (d\sigma/d\theta)_i\ d\Omega$.

$N_i$ is the density of scattering centers, $n_i$ the number of atoms per molecule, $Z_i$ the atomic charge and $p_i$ the partial pressure of species i. The corresponding differential scattering cross section is $(d\sigma/d\theta)_i$ and $\Omega$ is the solid angle over which particles are scattered out of the ring acceptance. c is the velocity of light .

When an elliptic machine acceptance with half-axes **a** and **b** is assumed and provided the pressure is reasonably uniform around the circumference, the expressions for $S_i$ and $\tau_{sc}$ become[26]:

$$S_i = (4 r_o^2 Z_i^2/\gamma^2)\ I(\Omega) \quad , \quad 1/\tau_{sc} = (4 r_o^2 K_n/\gamma^2)\ I(\Omega) \sum_i Z_i^2 n_i p_i \qquad (38)$$

with $I(\Omega) = (\pi/2)[(\beta_X \beta_{XM}/a^2) + (\beta_Z \beta_{ZM}/b^2)]$ .

$\beta_X$, $\beta_Z$ are the average values of the radial and vertical beta functions around the ring and $\beta_{xM}$, $\beta_{zM}$ their maximum values. Normally one also sets

$$\sum_i Z_i^2 n_i p_i \approx p Z^2_{eq} \qquad (39)$$

with p the total pressure. Normally $Z_{eq} \approx 7 \div 10$.

If the aperture limit is set by the beam dynamics and the maximum acceptance is $N_x\sigma_x$ , $N_z\sigma_z$ then I(W) in Eq. (38) can be written:

$$I(\Omega) = (\pi/2)[(\beta_X/N_x^2\varepsilon_x) + (\beta_z/N_z^2\varepsilon_z)] \qquad (40)$$

$\varepsilon_X$ and $\varepsilon_Z$ being the radial and vertical beam emittances.

### 4.3.2. Bremsstrahlung Lifetime

Bremsstrahlung in the field of residual gas atoms, or of their electrons, changes the particle energy; if the energy change is larger than the momentum acceptance, $(\Delta p/p)_{max}$, determined either by nonlinearities or by the RF bucket , the particle is lost.

To the accuracy required for an estimate of the lifetime, $\tau_b$ is given by:

$$1/\tau_b = (16/3)\, c\, K_n\, (r_o^2/137)\, (-\ln(\Delta p/p)_{max} - 5/8\,)\, \Sigma_i \ln(183/Z_i^{1/3})\, n_i\, p_i\, Z_i\, (Z_i+1) \quad (41)$$

or, with the approximation (39):

$$1/\tau_b = (16/3)\, c\, K_n\, (r_o^2/137)\, (-\ln(\Delta p/p)_{max} - 5/8\,)\, \ln(183/Z_{eq}^{1/3})\, p\, Z_{eq}(Z_{eq}+1). \quad (42)$$

Usually bremsstrahlung is not the dominant contribution to the lifetime of low emittance machines.

### 4.3.3. Touschek (or intrabeam scattering) Lifetime

Because of the single-Tousheck effect particles are scattered out of the machine momentum acceptance $(\Delta p/p)_{max}$. The scattering rate depends strongly on energy and on the particle density in the bunch: it is higher at low energies and high densities.

However, as the rate of single events increases, a multiple scattering regime sets in that causes the bunch volume to blow up until a steady state situation is reached. In addition, the bunch volume and therefore, for a given current, the density of particles, may also be determined by instabilities; typically the bunch length may be determined by longitudinal turbulence . As a consequence the particle density is a complicated function of current.

In general, therefore, Touschek lifetimes of SR machines have to be computed in a self consistent way, using complex programs such as ZAP[27] and the single-Touschek lifetimes produced by most general purpose lattice codes are not always meaningful .

## 4.4. The Effect of Insertion Devices on the Lattice Performance

### 4.4.1. General remarks

Even a perfect insertion device (ID) has a number of effects on the lattice parameters:

- it changes the tunes. For a planar device with vertical fields the vertical tune is the most affected;
- it can either increase or reduce the beam emittance depending on the value of the dispersion at the place where the device is inserted;
- it broadens the beam energy spread;
- it shortens the damping time;
- it shortens the beam polarisation time. Polarisation can also be rotated using special undulator arrangements [9,10].

Most effects are essentially proportional to the device strength parameter, K, to some power and to the device overall length. The perturbations induced by a perfect undulator are therefore in general negligible with respect to those produced by a perfect wiggler having the same length.

In the following it is generally assumed that wigglers and undulators are placed in dispersion-free sections.

The results of tune shift measurements on the ADONE wiggler[28] are compared to the computed values in Fig. 11. A simple linear calculation of the focusing perturbation introduced by an alternating magnetic field placed in a straight section was originally given in Ref. [29]. The effect of the ID, in a rectangular field approximation , is represented by a thin lens placed at the center of the straight section. The thin lens matrix phase shift and self-$\beta$ are $\theta^*$ and $\beta^*$ respectively. $\theta^*$ and $\beta^*/L$ , where L is the ID length, are universal functions of $B_o/B_{lim}$ where $B_o$ is the ID magnetic field and $B_{lim}$ is the value of $B_o$ at which $\theta^*$ approaches $\pi$ (see Fig. 12). $B_{lim}$ is given by:

$$B_{lim} = \pi/(cLf^2) \tag{43}$$

with $$f^2 = (\int |B_o|\, ds)/(B_o\, \lambda_{ID}).$$

If the unperturbed value of $\beta$ at the center of the straight section is equal to $\beta^*$, the ID is perfectly matched into the lattice.

The formulation is very useful to gain insight on the physics; in practice however matching conditions are computed numerically and implemented by changing the excitation of the ring quadrupoles. Furthermore, even under perfect (linear) matching conditions the machine periodicity is disturbed and the effect of nonlinearities, in the machine and in the device itself, has to be carefully evaluated (see for instance Ref. [25] ).

### 4.4.2. The Effect of Insertion Devices on the Damping Time

In general for a ring of energy E, bending radius $\rho$ and circumference $2\pi R$, the damping time $\tau$ is:

$$\tau_i = 4\pi T_0/(C_\gamma I_2 J_i \gamma^3) = \tau_0/J_i \tag{44}$$

with: $C_\gamma = 8.85\ 10^{-5}$ m.GeV$^{-3}$, $T_o$ the revolution period, $J_i$ the damping partition number and i=x,z, E. One has:

$$J_x = 1 - (I_4/I_2) \quad , \quad J_z = 1 \quad , \quad J_E = 2 + (I_4/I_2) \tag{45}$$

with $$I_4 = \int D_x G\,(2k + G^2)\, ds.$$

For uniform field bending magnets $(I_4/I_2)$ is usually « 1 , so that

$$J_x \approx 1 \quad , \quad J_y \approx 1 \quad , \quad J_E \approx 2 .$$

If the lattice is also isomagnetic , defining $R = F_m \rho$ , one has:

$$\tau_{o(s)} = K_\tau ( F_m \rho^2 / E^3 ) \qquad (46)$$

with $K = 4.74\ 10^{-4}\ s{\cdot}GeV^3/m^2$ .

For low emittance storage rings $F_m$ is usually quite small, typically of the order of .3 or less.

In the presence of wigglers/undulators, the ratio of perturbed ($\tau_w$) to unperturbed ($\tau$) damping time is:

$$\tau_w/\tau = (1+I_{2w}/I_2)^{-1} \qquad (47)$$

where $I_{2w}$ is the integral $I_2$ taken over the wiggler magnet length. $I_{2w}/I_2$ is always > 0, so that the damping time is always shortened.

### 4.4.3. Effect of the Insertion Devices on the Beam Energy Spread

The standard deviation of the beam relative energy spread is:

$$\sigma_E^2 = (C_\gamma \gamma^2/J_E){\cdot}( I_3/I_2) \qquad (48)$$

or, for an isomagnetic lattice:

$$\sigma_E^2 = Cq\ \gamma^2 /J_E\rho. \qquad (49)$$

In the approximation: $J_x \approx 1$ , $J_y \approx 1$, $J_E \approx 2$, the ratio of perturbed to unperturbed energy spread then becomes:

$$(\sigma_{EW}/ \sigma_{Eo})^2 = (1+I_{3w}/I_3) / (1+ I_{2w}/I_2) \quad , \quad I_3 = \int |G^3| \, ds \, . \qquad (50)$$

The energy spread is always increased.

### 4.4.4. Effect of Insertion Devices on the Beam Emittance

The ratio of perturbed to unperturbed emittance is given by :

$$(\varepsilon_{xw}/ \varepsilon_{xo}) = (1+I_{5w}/I_5)^* (\tau_w/ \tau_o), \qquad (51)$$

where $I_{5w}$ is the integral $I_5$ computed over the wiggler magnet. It is seen from (51) that the emittance can be either reduced or increased depending on the value of the integrals $I_5$ and $I_{5w}$.

When the dispersion in the straight section is zero, $I_{5w}$ is zero and the stronger damping causes

the emittance to decrease until the self-generated dispersion starts to take over (see below). When instead a strong wiggler is placed in a dispersive straight section the ratio $(I_{5w}/I_5)$ tends to become large and the emittance increases.

As said above, wigglers are usually placed where $D_x$ is nominally zero and $\beta_x$ is low. However the dispersion generated by the wiggler itself has to be taken into account. The value of $<H_w>$ for a sinusoidal field is approximately given by:

$$<H_w> = (D_x^2/<\beta_x>)+<\beta_x>(\theta_w^3)/5 \qquad (52)$$

with $\theta_w = K/\gamma$.

The two terms in (52) are the lattice and the wiggler contribution respectively. The first of course vanishes with Dx. $<\beta x>$ is the average of the beta function over the wiggler and is assumed to vary not too rapidly with s. Last, although the nominal value of $D_x$ is zero in the straight section, a residual dispersion due to misalignment and field errors will exist and may easily become the dominant term.

### 4.4.5. **Longitudinal Stability**

Small emittance lattices usually have very small values of the (linear) momentum compaction, $\alpha_c$. This because the integral defining it

$$\alpha_c = \int [D_x(s)/\rho(s)]\ ds$$

is closely related to Eq. (25) defining the emittance.

Values of $\alpha_c \approx 10^{-4}$ are not unusual for lattices with emittances $\approx 10^{-9}$ m rad. Nonlinear terms have therefore to be carefully evaluated because a highly nonlinear motion in the longitudinal phase space can lead to the loss of longitudinal stability[30].

### 4.4.6. **Ion Trapping**

An electron beam can, under certain circumstances, trap the positive ions it creates in the residual gas. The ions see the bunched electron beam as a sequence of focusing lenses[31]. Depending on the bunch charge, the pattern of bunches around the ring and the charge-to-mass ratio of the ions, the system can be stable (trapping) or unstable (no trapping). Trapped ions, besides possibly altering the local residual gas pressure, produce strongly nonlinear fields that can drive resonances, instabilities and coupling of the vertical to the horizontal motion, thereby increasing the emittance, lowering the lifetime and, in general, leading to less stable beams.

For very low emittance lattices one would generally predict ion trapping to be impossible or easily avoidable under most operating conditions. However the phenomenon is in practice very complicated and the theory in qualitative agreement only with the presently available experimental results. Furthermore, few data exist for rings with the kind of performance one is considering for

third generation machines. Given that the achievement of the design brilliance, long lifetime and stable, reliable operation are the main justifications for building advanced sources, positron beams (that can not trap the positive ions) are often considered by the designers of SR machines, in spite of the higher cost of positron injectors.

## REFERENCES


[1] J.Als-Nielsen, The case for a European Synchrotron Radiation Facility, ESF Strasbourg, (1982).
[2] G.Brown, SSRL, (1984).
[3] S.Guiducci, M.A.Preger, ADONE Int.Rep. G-41 (1981).
[4] A.Hofmann, Phys.Rep. 64, n.5, (1980).
[5] R.Barbini et al., The Adone Wiggler Facility, N.Cim., 4, n.8, (1981).
[6] R.Coisson, ESRP Report IRM-34/84.
[7] R.Coisson, LNF Int. Rep. 85/32 (R).
[8] K.J.Kim, Nucl. Instr. & Meth., A219, 425 (1986).
[9] K.J.Kim, Nucl. Instr. & Meth., A246, 67 (1986).
[10] J.Goulon, P.Ellaume, D.Raoux, Nucl. Instr. & Meth., A254, 192 (1987).
[11] K.Halbach, IEEE Trans.NS , NS-26, 3882 (1979).
[12] K.Halbach, J. de Phys., MT-8, C1-211 (1981).
K.Halbach et al., IEEE Trans.NS., NS-32-5, (1985).
[13] R.Coisson and R.P.Walker , Proc. of SPIE , 582 , 24 (1985).
K.J.Kim, Proc. of SPIE , 582 , 2 (1985)
[14] R.Coisson, S.Guiducci, M.A. Preger, Nucl. Instr. & Meth., 201, 3 (1982).
[15] M.Sommer, LAL Int. Rep. RT/83-15, DCI/NI/20-81.
[16] L.C.Teng, Fermilab Int.Rep. LS-17, (1985).
[17] A.Wruhlich, LBL Preprint LBL-21215 (1986) and Part. Acc.
[18] G.Vignola, in Part. Acc., 18 , n.4,223, (1986).
A. Jackson , LBL Preprint LBL-21279 (1986) (Submitted to Part. Acc.).
[19] C. Biscari, L. Palumbo, LNF- Adone Int. Memo G-76 (1986), G-77 (1986).
M. Biagini, C. Biscari , LNF- Adone Int. Memo AF-14, (1986).
[20] D.Einfeld, G.Muehlhaupt, Nucl. Instr. & Meth. 172, 191 (1980).
[21] For extensive reviews see: Proc. Workshop on Accelerator Orbit and Particle Tracking Programs, Informal Report BNL-31761, (1982); Proc. 1985 Sardinia Workshop on Nonlinear Dynamics Aspects of Particle Accelerators, ed. by J.M. Jowett, M. Month and S. Turner, Springer Verlag, Lect. Notes in Phys., 247, Berlin (1985).
[22] M. Bassetti, DESY Int. Report PET-77/35 (1977) and LNF Int. Report T-95.
[23] The ESRF Foundation Phase Report, February 1987, European Synchrotron Radiation Facility, Grenoble.
[24] J.M. Jowett, Slac-Pub-3987.
[25] Proc. Magnet Errors Workshop, Ed. By J. Murphy and M. Cornacchia, Brookhaven, (1986).
[26] C. Bernardini et al., Proc. Dubna Intern.Conf.on H.E. Particle Accelerators, Dubna, 332, (1963).
[27] M. Zisman, S. Chattopaddhyay, J.J. Bisognano, LBL Report, LBL-21270 and UC-28 (1986).
[28] R. Barbini et al., Rivista Nuovo Cimento, 4 , n° 8 (1981).
[29] M. Bassetti, S. Tazzari, Proc. Wiggler Meeting, ed. by A. Luccio, A. Reale and S. Stipcich, Frascati (1978).
[30] B.Buras, S.Tazzari, Report of the ESRP, c/o CERN, Geneva (1984).
[31] Y.Baconnier, G.Brianti, CERN Report CERN/SPS/80-2(D1).
M.E.Biagini et al., Proc. XIth Int. Conf.on H.E. Particle Accelerators, CERN, Geneva (1980).